Chapter 4

Bare Si Surfaces

4.1 Introduction

Surfaces and interfaces of semiconductors play an important role in technological device applications. Their physical and chemical characteristics are responsible for the interesting properties and making them an active area in semiconductor research.

This chapter focuses on the low index (001) and (111) surfaces of silicon. The surface structure, surface free energy and the electronic properties of the clean surfaces are discussed.

Silicon with diamond structure is characterized by four strongly covalent bonds. Each bond holds two spin-paired electrons. The surface can be prepared by cutting the crystal in a certain orientation. During the surface creation, at least one bond per atom will be cut upon cleavage, which is called ”dangling bond”. The unsaturated dangling bonds make the surface unstable and are responsible for an increase in the surface free energy. A reduction in the number of dangling bonds minimizes this energy and is the driving force behind the surface relaxation and reconstruction. With the atomic displacement in surface relaxation and reconstruction this energy can be minimized. The atoms seek to find new positions which reduce the number of the dangling bonds.

Upon *relaxation* the atoms at the surface are displaced from their bulk positions, but there is no change in the surface periodicity or symmetry. The *reconstruction* of a surface, on the other hand, involves a change in the surface unit cell, compared to an ideal or bulktruncated surface, thereby leading to a change in the periodicity and symmetry at the surface.

There are two basic principles which can explain the surface reconstruction and re-

laxation. Duke [89] has presented them in detail for the tetrahedrally coordinated compound semiconductors:

Principle 1: Reconstructions tend either to saturate surface dangling bonds via rehybridization or to convert them into non-bonding electronic states.
Surface reconstructions minimize the number of the dangling bonds by the formation of new bonds between neighboring surface atoms via hybridization. This leads to a fully occupied or unoccupied energy state which in Si(001) transforms the metallic character of the unreconstructed surface to a semiconductor one.
Principle 2. In many cases surfaces can reduce their energy by both atomic reconstruction and relaxation.
For example in Si(001), the atom relaxed toward the bulk (with conserving the surface symmetry) donates the electronic charge in its dangling bond to couple with the dangling bond of a neighboring atom, which has relaxed away from the bulk. The atomic relaxation will not change the symmetry of the surface .

Different surfaces of a crystal have different surface free energies, depending on their orientations. The most stable surface is the one, which exhibits the lowest surface free energy. The surface free energy at zero temperature is given by:

$$\gamma^{\mathrm{SUR}} = \frac{E^{\mathrm{slab}} - \sum_i N_i \times \mu_i}{2 \times A} \tag{4.1}$$

where E^{slab} is the total energy of a slab calculation with two identical surfaces, μ_i is the chemical potential of the surface constitute components, N_i is the number of the ith kind of atoms per unit cell and A is the unit cell area. There are two surfaces in the slab model therefore, the factore $\frac{1}{2}$ is applied.

4.2 Si(001) Plane

The Si(001) surface has received particular attention for two reasons. Firstly, most silicon devices are grown on this substrate and secondly, because it has the most simple reconstruction, compared to other silicon surfaces. The characteristic feature of this surface are the Si-dimers, which have been studied with a large variety of experimental and theoretical methods.

In 1959, Schlier and Farnsworth [90] used low energy electron diffraction (LEED) technique and were the first to observe a (2×1) periodicity (cf. Fig. 4.1-b) on the this surface. In such a periodicity, surface atoms come together to form dimers,

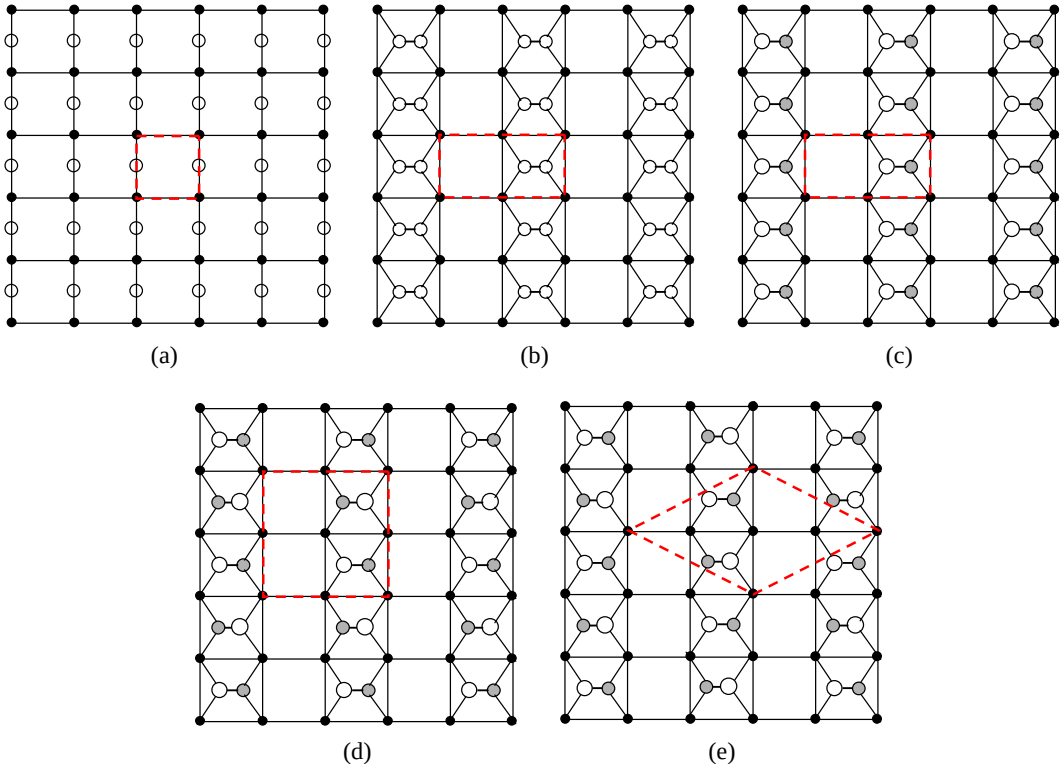

Fig. 4.1: Top view of different unit cells at the (001) surface for which we have calculated the surface energy. White circles show atoms in the surface layer and black circles represent atoms in the second layer but big white and small gray circles are used to show upward and downward buckled dimer atoms on the surface, respectively. The non-reconstructed surface (a), the (2×1) symmetric dimer reconstruction (b), the $p(2\times1)$ buckled dimer reconstruction (c), the $p(2\times2)$ alternating buckled dimer reconstruction (d), the $c(4 \times 2)$ reconstruction (e).

thereby reducing the surface energy. The formation of dimers halves the density of dangling bonds compared to a bulk terminated surface. Dimerization, as a basic reconstruction, was observed also in photoemission experiments [91], optical observations [92], core-level spectroscopy [93] and scanning tunneling microscopy (STM) [94]. One of the first calculations on dimerized surface was performed by Appelbaum and Hamann in 1974 [95]. They showed that the dimer length are slightly shorter than the distance of atoms in the silicon bulk and that the subsurface distortion due to surface dimerization extends up to 4-5 layers into the bulk [95]. This model predicted a metallic band structure, contrary to experimental observations. The reason for this discrepancy is that in a symmetric dimer model, one dangling (or unsaturated) bond per surface atom remains, leading to a metallic surface.

The symmetric dimer in Si(001) is energetically unstable, therefore Chadi proposed that the buckled dimer surface is the most stable surface of Si(001) [96]. Support for

the dimer buckling came from ion scattering measurements [97, 98] and STM [94], which confirmed Chadi's prediction. Apart from an energy gain, the buckling of the surface dimer is accompanied with the formation of a semiconducting electronic band structure [96]. The charge transfer between the dangling bonds causes one dangling bond per dimer to become completely filled while the other one is empty. This opens the gap in the band structure of the (2×1) asymmetric model. The bonding geometry of the Si atom relaxed towards the bulk becomes more planar. Therefore, its orbital hybridization changes from sp^3 to sp^2. Its dangling bond gains more p character and becomes unoccupied. The dangling bond of the other Si dimer atom (the one relaxed outwards) becomes fully occupied [99]. The π bond found between Si atoms of the symmetric dimer is partially destroyed by buckling, but the energy gain due to the rehybridization mechanism obviously overcompensates this energy cost [89].

Due to elastical coupling via the atoms in the second and deeper layers the buckling angle alternates along the dimer row. The lowest energy reconstruction is $p(2 \times 2)$ or, even slightly lower, $c(4 \times 2)$.

A top view of the various reconstructions on the Si(001) surface is shown in Fig. 4.1. The calculated geometric (atom displacement, dimer lengths, dimer angles) and electronic (surface free energy, bandstructure) properties of this structures, i.e. the (1×1) ideal, the (2×1) symmetric dimer, the (2×1) asymmetric dimer, the $p(2 \times 2)$ alternating buckled dimer and the $c(4 \times 2)$ reconstruction, cf. Fig. 4.1, are discussed in the following sections.

4.2.1 (1×1) Non-Reconstructed

In the ideal Si (1×1) surface termination, every silicon atom remains in its bulk position, but has only two-fold coordination. The calculated surface energy is 2.05 eV per (1×1) unit cell. The generation of this surface structure upon cleavage of the Si bulk leads to the formation of two surface state bands in the band gap of bulk silicon, that cut the Fermi level. These surface states are not localized and the bands is highly disperse, which shows significant overlap between states of surface atoms. These surface states are responsible for the metallic character of Si.

These two dangling bonds make the surface unstable, therefore the surface atoms move close to each other to form one bond which creates the dimerized (2×1) reconstructed surface.

4.2.2 (2×1) Dimer Model: Symmetric/Asymmetric Si Dimers

The surface energy for the symmetric and the asymmetric dimer reconstructions are 2.74 eV / dimer and 2.59 eV / dimer, respectively. They are 1.37 eV and 1.52 eV / (1×1) unit cell lower than the unrelaxed ideal surface. The dimer bond length is 2.30 Å for symmetric and slightly longer, 2.32 Å , for asymmetric dimer structure while the bond length of the bulk silicon is 2.37 Å . The vertical distance separation between the up and the down atom of the dimer is 0.74 Å and the angle of the buckled dimer is 18.7° which is comparable with the angle of 18.3°, reported by Ramstad, Brocks and Kelly [100] and 15° reported by Dabrowski and Scheffler [101]. The angle of the buckled dimer extracted from the analysis of transmission electron diffraction (TED) measurements, 7°, [102] and a X-ray diffraction, 5°, [103] are substantially smaller than calculated values. In contrary, low-energy electron diffraction (LEED) at low temperature (120 K) gave a value of 19° for the tilt of the dimer [104]. All bond lengths for these reconstruction are shown in Fig. 4.2.

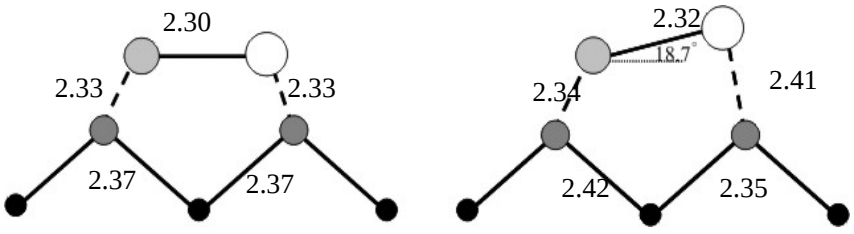

Fig. 4.2: Bond length of symmetric dimer structure (a), the bond length and the angle of the buckled dimer structure (b).

The discussed results are for calculations performed at temperature of $0\,K$, therefore they should be compared to the low temperature experimental geometry. According to STM experiments at room temperature [94], the dimers appears to be symmetric. It has been suggested that the symmetric images are caused by the thermal flipping motion of the dimers between the left and the right tilted position [105]. In fact, asymmetric dimers have been observed in low temperature STM experiments [105, 106].

In the dimer model, the equivalent dangling bond orbital of each dimer atom are coupled by π interaction. The bandstructure is shown in Fig. 4.3. The projected bulk band structure is shown as a gray shaded area. The π states are split into a bonding π-band and an anti bonding π^*-band. One thing to notice in this figure is

that all bands come in pairs. This is a consequence of using a slab model, i.e. there are actually two surfaces. In an infinite thick slab, these pairs would be degenerated.The small energy splitting remains because of the finite thickness. Simple solution to this problem, is to take the average of the split pairs. However, the features of the electronic structures is reasonable and will not substantially change when the thickness of slab is increased.

The rather strong interaction between neighboring dangling bonds in the symmetric dimer leads to a significant dispersion of the bands. In fact, the dangling bonds on the Si(001) surface have itinerant electron, which causes the metallic character in the band structure of this surface. The formation of an asymmetric dimer is associated with a charge transfer of 0.36 from the atom which moves downward to the atom which is shifted up [96]. This charge transfer from the down to the up atom in the asymmetric configuration results in the formation of a partly ionic π bond between two atoms, leading to a downward shift of the π and upward shift of the π^* band.

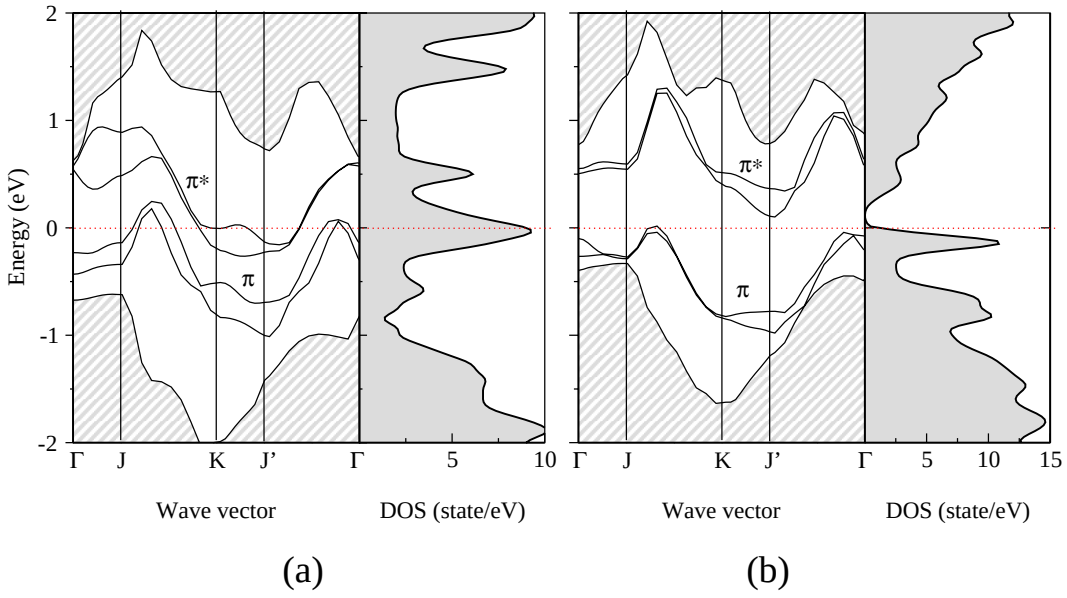

Fig. 4.3: Band structure and density of states for (2×1) symmetric (a) and asymmetric (b) dimer. The band structure and DOS of the symmetric dimer has metallic character while the Fermi level cuts the tail of DOS and touches the top of valence band. The shaded areas in the band structure correspond to the highest valance band or the lowest conduction band in the slab.

The dispersion of surface bands is almost the same for both the symmetric and the asymmetric dimer. The band width is around 0.7 eV which is close to the experimental value of 0.65 eV [107]. There are large changes in the π^* states mainly in

$K \rightarrow \mathrm{J}'$ direction which is parallel to the dimer bonds.

There is a pronounced splitting between the π and π^* energy bands in the asymmetric structure, leading to the formation of a band gap, slightly above the Fermi level. As can be seen in the DOS plot, the Fermi level cuts the tail of valance band. The width of the calculated band gap is 0.1 eV. It is significantly smaller than the experimentally measured band gap. A band gap of 0.9 eV (corresponding to the indirect gap from Γ to **k**) was measured using scanning tunneling spectroscopy [107, 108], while the value obtained from angle-resolved photoelectron spectroscopy (ARUPS) is 0.7 eV. On the other hand, a direct band gap of 1.7 eV was obtained by Rowe and Ibach with electron energy loss [109].

The underestimation of band gaps is a well-known shortcoming of LDA calculations. For Si surfaces, this flaw is also not corrected within GGA. To further understand if there is a relationship between the structural stability of different reconstructions and the existence of a band gap or region of low densities of states, the band structures of various reconstructions are compared.

4.2.3 Alternating Buckled Dimers: $p(2 \times 2)$/$c(4 \times 2)$ Supercells

It turns out that the formation of an asymmetric dimer leads to a significant amount of mechanical stress at the surface. This surface stress can be partially released if the dimers are buckled in alternating form which reduces the surface energy. Different orders of arrangements of these buckled dimers give the p(2×2) or c(4×2) reconstructions. These are the most stable reconstructions on the Si(001) surface. The buckled dimers alternate either in one direction with $p(2 \times 2)$ unit cell or in two directions with $c(4 \times 2)$ unit cell. In other words, in the $p(2 \times 2)$ structure, the direction of buckling alternates along the dimer rows while in the $c(4 \times 2)$ reconstruction they alternate both parallel and perpendicular to the dimer rows .

The buckled dimers first appear on the surface at 120 K and their number increases with decreasing temperature [110]. At low temperature ($\sim$ 4 K) there is transition from the $p(2 \times 2)$ to the $c(4 \times 2)$ reconstruction. The occupied area by the $c(4 \times 2)$ phase is larger than the part with $p(2 \times 2)$. [106]. The barrier to flip the dimer is about 0.1 eV [48, 111].

The calculated surface energy for the buckled structure is 2.503 eV per dimer which is almost the same for both reconstructions. The surface energy of the $c(4 \times 2)$ reported in the literature is slightly ($\sim$ 2 meV / dimer) lower than for the $p(2 \times 2)$ structure [100, 112], which is not noticeable in theses calculations.

The dimer bond length of 2.38 Å is almost the same for both structures, while the tilt angle of the dimer in the $c(4\times2)$, 18.7°, is slightly larger than that in the $p(2\times2)$ structure, 18.3° (cf. Fig. 4.4). The up and down atom on the dimer are separate by a vertical distance of 0.73 Å in the $p(2\times2)$ and 0.96 Å in the $c(4\times2)$ structures, respectively. This is shorter than the vertical distance between atoms in the bulk which is 1.37 Å. The dimer bond lengths and the back-bond lengths (the bonds between the dimer atoms and those in the second layer) is given for each of these structures Fig. 4.4.

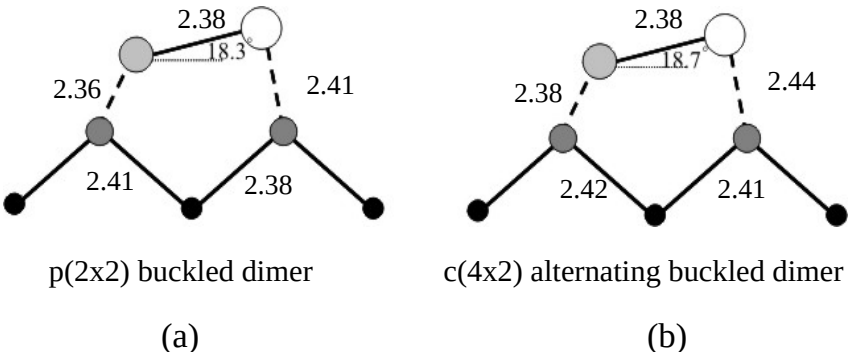

Fig. 4.4: Bond length and the angle of the alternating buckled dimers structure in p(2×2) (a), and c(4×2) (b) supercells.

In the figure 4.5, we present our results of calculated surface energies of different reconstructions. A difference of 0.2 eV / dimer between the energy of symmetric and asymmetric dimer reported in the literature is the result of a pseudopotential calculation [100]. This value is larger than the one which is calculated here (cf. 4.5). Furthermore, the surface energy of the $p(2\times2)$ buckled structure is reported to be 0.02 eV / dimer lower than the (2×1) asymmetric dimer [100]. A small energy difference of 1-2 meV / dimer between the $p(2\times2)$ and the $c(4\times2)$ reconstruction is reported by Inoue *et al.* [112] and Ramstad *et al.* [100], but no such difference is observed in the present calculations.

In the following, the electronic structure of the alternating buckled dimer structures are discussed. The density of states and the band structure of the $p(2\times2)$ and $c(4\times2)$ structures are shown in Fig. 4.6.

The band structure of the $c(4\times2)$ reconstruction was calculated using a (4×2) unit cell, ensuring that there are eight surface atoms in the cell and corresponding eight surface bands in the band structure plot. Similarly, the four surface atoms per $p(2\times2)$ unit cell, are responsible for the appearance of four surface states in the bulk band gap for that reconstruction. These four states are derived from the

four dangling bonds, two with π character (π_1 , π_2), which are occupied, and two π^* antibonding states (π_1^* , π_2^*), which are empty.

Due to the buckling of the dimer in the $p(2\times2)$ and $c(4\times2)$ structures, the dispersion of the surface bands are about 0.6 eV for the occupied states and about 0.8 eV for unoccupied state compared to the (2×1) structure. The valence band of the $c(4\times2)$ is shifted downward by about 0.2 eV, increasing the band gap, and the surface bands become smoother compared to the $p(2\times2)$ structure.

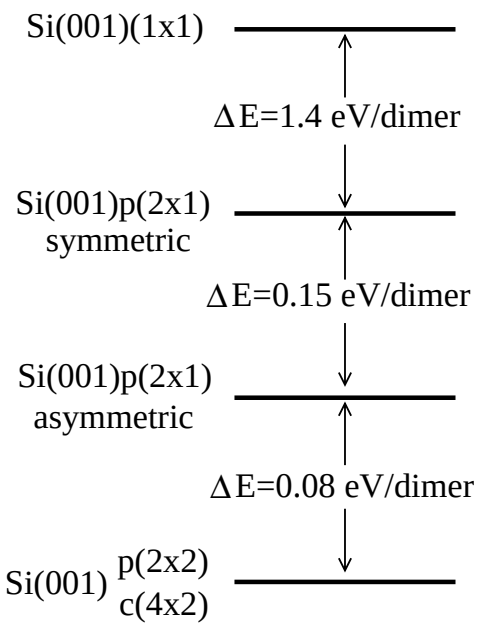

Fig. 4.5: Calculated energy difference between all possible surface reconstructions of the Si(001) surface.

The DOS plot and band structure of $p(2\times2)$ and $c(4\times2)$ structures are shown in Fig. 4.6. The significant changes appear in the occupied states (especially in the directions perpendicular to dimer rows). The less dispersion of the bands open larger gap in the band structure in comparison to asymmetric (2×2) reconstruction. In the alternating dimer reconstructions the bandwidth of π band decrease which leads to a larger band gap. The lower energy of the $p(2\times2)$ and $c(4\times2)$ reconstruction can be associated with a increasing of the band gap.

The lowest energy of the π^* band is 0.3 eV (0.1 eV) above the valence band maximum (VBM) for $c(4\times2)$ ($p(2\times2)$) reconstruction. The corresponding experimental value obtained from optical absorption experiments is about 0.4 eV [92]. The two unoccupied states (π_1^* and π_1^*) are separated by 0.5 eV in the $c(4\times2)$ structure and 0.7 eV in the $p(2\times2)$ structure at the Γ point where the minima of unoccupied states are located. The dispersion in the $\Gamma\rightarrow$ J and $K\rightarrow$ J$'$ directions (along dimers bonds) is flat in both structures. The valence band at the Γ point is 0.3 eV below the Fermi level, which is half of the value measured by ARUPS, being 0.6 eV [113].

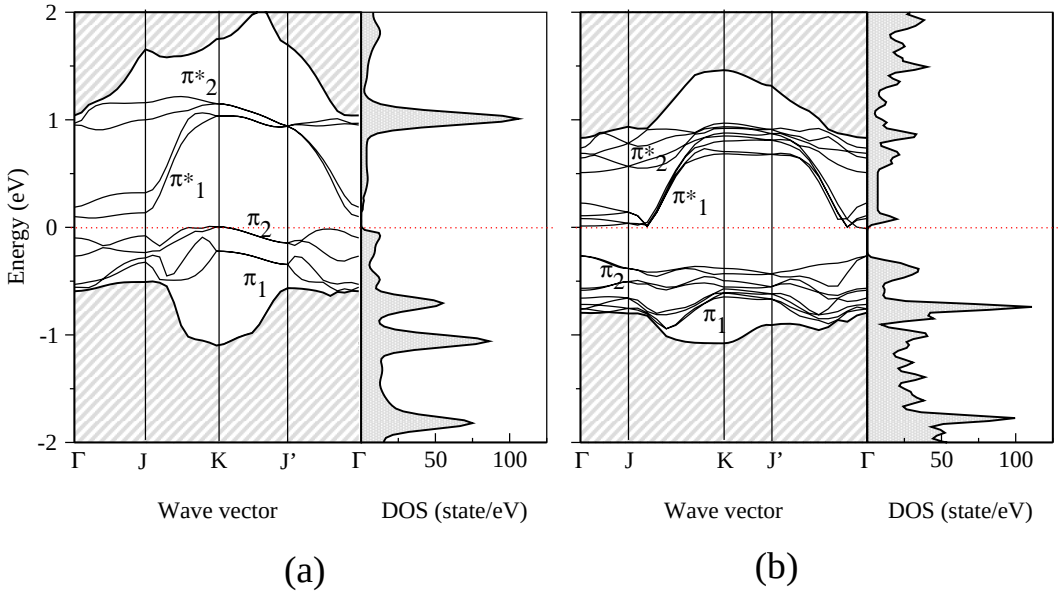

Fig. 4.6: Band structure and density of states for $p(2\times 2)$ (a) and $c(4\times 2)$ (b) reconstruction. The band structure of the $c(4\times 2)$ reconstruction was calculated using a (4×2) unit cell.

- **Scanning Tunneling Microscopy (STM)**

In order to compare simulations with experiment, the reconstructed structures of the Si (001) surface in the low temperature regime where the flip-flop motion of dimers is frozen, are considered. As is evident in Fig. 4.7, which shows the simulated and experimental STM pictures of the $c(4\times 2)$ and $p(2\times 2)$ reconstruction, the simulated images accurately reproduce the experimental result. The experimental images were produced at a temperature of 4.2 K, using a positive sample bias of 1.3 eV (2 eV) for the $c(4\times 2)$ ($p(2\times 2)$) structure and a tunneling current of 30 nA .

As shown in Fig. 4.7, the simulated images can support the interpretation of the experimental STM images. The simulated images are generated from the electronic local density of states of 10^{-5} electrons / Å ^{3} (0.5×10^{-5} electrons / Å ^{3}) for the $c(4\times 2)$ ($p(2\times 2)$) structure. The estimated distance from the surface at the mentioned charge density is at a height 4 – 4.7 Å above the surface in a (2.3×2.3) nm^2 scan region. The applied voltages are 0.5 eV above the surface Fermi level corresponding to the empty states of the surface. In these images the gray-scale range from bright to dark represents a height change of around 4 Å.

In the experimental $c(4\times 2)$ image, Fig. 4.7-a, the buckled dimers form a honeycomb pattern while in the $p(2\times 2)$, Fig. 4.7-d, the dimer rows have a zigzag shape. It is found, that at low temperature the out of phase $c(4\times 2)$ arrangement is prefer-

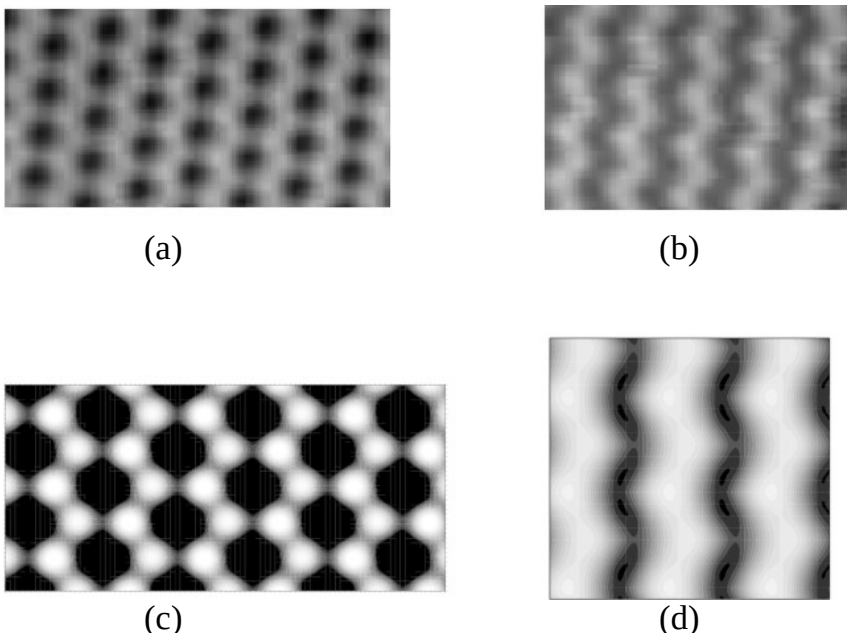

Fig. 4.7: Simulated and experimental empty states images for $c(4 \times 2)$ structure (a, c) and $p(2 \times 2)$ structure (b, d). The experimental images are measured with a positive sample bias of 1.3 eV and 2 eV for the mentioned structures.

entially formed. The domains with in-phase $p(2 \times 2)$ order are five times less than the $c(4 \times 2)$ areas [110].

Looking at the $p(2 \times 2)$ structure, one protrusion is clearly distinguished inside one buckled dime. This bright part belongs to the upper atom Fig. 4.7-d. The dark areas are surface depressions where the dangling bonds in the deeper layers are lacking. This bean-like shape of bright parts was reported for first time by Hamers $et\ al$ [105].

4.2.4 Dimer Vacancy

Thirty years ago it had been suggested that the energy of the Si(001) surface would be lowered if a small fraction of the dimers were removed from the surface. Due to the dimer vacancy, the atoms below could rebond, eliminating two dangling bonds for every dimer involved. Later on, it was shown by Robert and Needs, that the strain due to the dimer vacancy would prevent the atoms below to rebond [114]. In order to study the effect of a vacancy on the surface stability, calculations for one dimer vacancy were performed for (2×4) and (4×2) unit cells.

The two considered defect geometries are shown in Fig. 4.8. The energy cost to form a defect in the (4×2) and the (2×4) structure is 0.52 eV / dimer and 1.0 eV / dimer,

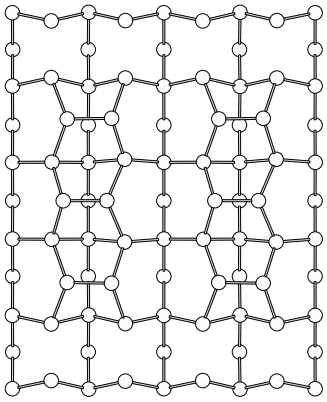

1 dimer defect in (2x4) cell

(a)

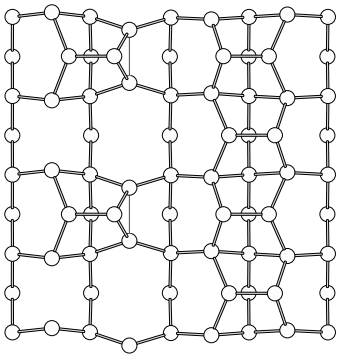

1 dimer defect in (4x2) cell

(b)

Fig. 4.8: Top view of (2×4) (a) and (4×2) (b) surface unit cell containing one dimer vacancy.

respectively. In the (2×4) geometry the vacancy structure is obtained by removing one dimer in every fourth dimer at the surface. This results in an ordered array consisting of one empty site and three dimers in each cell (cf. Fig. 4.8-a). The neighboring dimers become shorter in the (2×4) structure (by 0.08 Å), the angle of buckling is reduced to 15° and the atoms of these dimers are pulled downwards (by 0.3 Å) towards the defect. Simultaneously the exposed second-layer atoms beneath the defect move closer together until their sparation distance is 2.94 Å which is about of 1.22 Å (i.e. 30%) shorter than for the second-layer atoms located below the dimer rows.

The energy cost to form a defect in a (4×2) cell equals half that of the (2×4) geometry. In the (4×2) structure, Fig. 4.8-b, there is one full dimer row, while every second dimer is removed in the adjacent row. The strain in this geometry is smaller than in the previously discussed structure, there is an additional bond of 2.61 Å between the second-layer atoms (the triangle in Fig. 4.8-b). These atoms in the second layer are pulled downward by 0.3 Å (compared to the second-layer atom below the full dimer row). The other second-layer atoms (these are below the lower dimer atom) approach each other and move toward the defect until they reach a distance of 4.32 Å from each other. The angle of dimers increases to 20° and 22° for the full and the defect containing dimer rows, respectively.

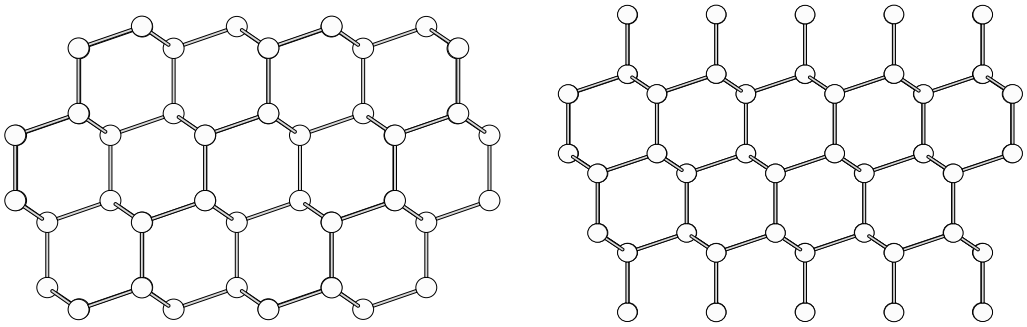

Shuffle terminated face (a)

Glide terminated face (b)

Fig. 4.9: Side view of the bare Si(111) surface. It has two possible terminations, the single-dangling-bond (SDB) which is called shuffle-terminated face (a), triple-dangling-bond (TDB) which is called glide-terminated face (b).

4.3 Si(111) Surface

The Si(111) surface is cleavage face of silicon for which the covalent bonds along [111] direction are cut. Depending on the number of layers, there are two surface terminations, see Fig. 4.9:

(a) Cleaving so that it has a single dangling bond (SDB) per surface atom which is called shuffle-terminated face [115, 116], see Fig. 4.9-a.

(b) Single coordination atop site, which has three dangling bonds (TDB) per surface atom which is called glide-terminated faces (cf. Fig. 4.9-b). Due to the degrees of freedom of the surface atom in all direction, this surface reconstructs.

It has been established that this surface has a 7×7 reconstruction as described by Takayanagi [1] [117]

There are also several surface reconstructions at different temperatures: Below T $\leq$ 600 K, cleavage produces a (2×1) structure, annealing this surface above 600 K generates a (5×5) structure which upon further heating to 870 K becomes a (7×7) structure [89, 118] . Still further heating to about 1120 K causes a phase transition to the (1×1) symmetry [119]. There are some studies which consider these structures and the transitions between them, that have been reviewed by Haneman [118]. Also the existence of metastable (9×9), (2×2), $c(4\times2)$ and $(\sqrt{3}\times\sqrt{3})$ reconstructions was observed by STM [120].

The triple-dangling-bond (TDB) face could theoretically be created upon cutting

[1] This model basically consists of 12 adatoms arranged locally in the 2×2 structure, nine dimers on the sides of the triangular subunits of the 7×7 unit cell and a stacking fault layer.

perpendicular to the (111) direction between the two narrowly spaced layers, in contrast to the single-dangling-bond (SDB) face, which separates the widely spaced bilayers at which the dangling bond is oriented exactly in the (111) direction. From this two possible cleavage planes, the SDB requires less energy since only one bond per atom has to be broken. Although cleaving along the TDB face involves the separation of three bonds, the surface energy is not three times as large as for the SDB surface. The present results for the surface energies confirm this trend. The calculations for the SDB and the TDB surface are performed using symmetric slabs of 12 and 10 atomic layers, respectively. Five (four) layers on each side are relaxed. Two layers in the middle of the slab are kept bulklike. The TDB termination is usually discarded for energetic reason since the cutting of three bonds needs more energy. The surface energy, γ, is 100.08 meV / Å^2 and 175.05 meV / Å^2 for the SDB and TDB, respectively. The surface energy for the TDB is only 0.98 eV / unit cell (1.75 times) higher than for the SDB surface.

The surface energy for the SDB termination using pseudopotentials gives a value of 108.6 meV / Å^2 for the (1×1) relaxed unit cell which decreases to 85 meV / Å^2 for the (7×7) reconstructed surface [121]. Using molecular dynamics with empirical potentials or tight-binding calculations leads to a value of 88.0 meV / Å^2 [122].

The relaxed structure for SDB (TDB) has an inward relaxation of the first atomic layer by a vertical displacement of 0.144 Å (0.005 Å) and an outward relaxation of the second layer by a vertical displacement of 0.035 Å (0.005 Å). The energy gain in the relaxed structure is due to the short bond between the atoms in the first and the second sub-surface layer which is contracted by 0.18 Å (18% shorter than unrelaxed bulk terminated).

On the SDB surface there is only a very weak π-like interaction of the dangling bond orbital over second nearest neighbor distance. The surface is metallic for both SDB and TDB surfaces.